JOURNAL OF GUIDANCE, CONTROL, AND DYNAMICS
Vol. 22, No. 3, May–June 1999

Multiple Rigid-Body Reorientation Using Relative Motion with Constrained Final System Configuration

David S. Rubenstein*
Charles Stark Draper Laboratory, Inc., Cambridge, Massachusetts 02139-3563
and
Robert G. Melton†
Pennsylvania State University, University Park, Pennsylvania 16802-1401

Moveable appendages in multibody spacecraft can augment or replace the attitude control actuators. In this work, motions of the movable bodies relative to the main body are used to adjust the system's inertial attitude so as to approach or attain a desired target attitude. A control algorithm designed to generate the maneuver commands that cause the necessary relative motions is tested with several cases representing a variety of dynamic conditions. The control can accommodate many different system configurations and dynamic conditions such as nonzero system momentum, a problem that historically has proved difficult to solve in a generalized, three-dimensional mode. Additionally, the control can return the system's geometric configuration to its initial state by the conclusion of the reorientation. The results indicate that the control can accomplish nearly complete reorientations in all cases tested while meeting the system constraints.

Introduction

ATTITUDE dynamics and control of multibody spacecraft have been studied extensively, including rigid-body/flexibility effects, time- and propellant-optimality, reachability of the target state, and computational approaches. Although by no means inclusive, Refs. 1–15 represent a broad sampling of these efforts. This paper focuses on the somewhat specialized problem of how to reorient a spacecraft by making use of any moveable appendages or sections of the vehicle. The need for such a strategy can arise when the primary attitude control system is partially disabled or could be augmented with this alternative control method.

The objective here is to design and simulate a method of rigid-body spacecraft reorientation, utilizing any existing movable appendages of the system, by means of nonlinear programming and an optimization algorithm that uses collocation.[16] Others[17,18] have successfully applied this control method to spacecraft attitude control problems involving constraints and objectives different from the system discussed in this work. The controller should be capable of accommodating reorientations of systems with various initial states of attitude and rate errors, although here only the attitude is controlled (i.e., it is assumed that the final rates are zero, although in principle they could be any desired values). Reorientation is accomplished by a sequence of strategic maneuvers of the connected movable rigid bodies so that the actual final system attitude at least approaches the desired final system attitude. Because relative motion of these bodies results in a change in the overall inertia tensor of the system, the angular rate also will change, maintaining constant system angular momentum. This change in angular rate is utilized to cause desired changes in attitude. It is assumed that in many, if not all, cases the controller will be unable to attain the exact desired orientation and that the extent to which the achieved attitude meets the desired attitude will depend on the particular case in question. For this reason, a success criterion was implemented that recognizes this constraint and requires only that the system at least be tended in the direction of the desired orientation.

Presented as Paper AAS 95-415 at the AAS/AIAA Astrodynamics Specialist Conference, Halifax, Nova Scotia, Aug. 14–17, 1995; received April 22, 1996; revision received May 28, 1998; accepted for publication Nov. 24, 1998.

*Senior Engineer, Guidance, Navigation, and Control Directorate.
†Associate Professor, Department of Aerospace Engineering. Associate Fellow AIAA.

To achieve the desired objective, one employs a modified version of direct collocation, which is capable of generating the approximate numerical control history to produce the desired reorientation. Additionally, a multibody simulation code verifies the effect of the control on the system. The results depict the ability of the control method to attain desired states, through a range of initial conditions as well as other system parameters that were varied to more accurately assess the validity of the approach. This work also demonstrates the ability to use collocation on modest-size computers with nonspecialized optimization software (i.e., routines not designed to handle large numbers of optimization parameters).

System Dynamics

The example chosen for this work is a three-body system with a main body (A) and two secondary bodies (B and C). Bodies B and C are attached to body A by means of gimbals, allowing rotational degrees of freedom only. Motion of the secondary bodies is used to manipulate the attitude of the system, as described by a reference frame fixed in the main body. Figure 1 depicts the configuration of the three bodies in this problem; Table 1 gives the mass properties of a representative spacecraft. This model is derived from the mass properties of a specific class of satellites that are still active and have multiple moveable rigid bodies. The gimbal between bodies A and B is assigned two angular degrees of freedom, with angles α and β, respectively. Body C is connected to body A via a gimbal with a single degree of freedom, denoted by the angle γ. The controller will generate maneuver commands in terms of α, β, and γ such that the system's inertial attitude is at least tended in the direction of the desired inertial attitude and such that each of the three gimbals is returned to its initial angular position. This is shown for a range of initial dynamic conditions. The results of the reorientation maneuvers are provided by several dynamic parameters extracted from the respective simulations.

Straightforward dynamic analysis leads to the equations of motion, which are written to provide the desired observable quantities and explicit terms in the necessary input parameters for the control. These equations are used in the simulation portion of the development to model vehicle attitude dynamics as well as in the control portion to compute vehicle angular rate at the necessary discretized points in the controller time history.

With reference to Figs. 2 and 3, the total system momentum can be written as

$$\boldsymbol{H}_T = \boldsymbol{I}_A \cdot \boldsymbol{\omega}_A + \boldsymbol{I}_B \cdot \boldsymbol{\omega}_B + \boldsymbol{I}_C \cdot \boldsymbol{\omega}_C + \boldsymbol{r}_A \times m_A \dot{\boldsymbol{r}}_A + \boldsymbol{r}_B \times m_B \dot{\boldsymbol{r}}_B + \boldsymbol{r}_C \times m_C \dot{\boldsymbol{r}}_C \tag{1}$$

where

$\boldsymbol{I}_A, \boldsymbol{I}_B, \boldsymbol{I}_C$ = inertia dyadics for bodies A, B, C (referenced to their respective mass centers);
$\boldsymbol{\omega}_A, \boldsymbol{\omega}_B, \boldsymbol{\omega}_C$ = angular rate vectors for bodies A, B, C (about their respective mass centers);
$\boldsymbol{r}_A, \boldsymbol{r}_B, \boldsymbol{r}_C$ = vectors from the combined system c.m. to the particular body c.m. for bodies A, B, C (Fig. 2);
m_A, m_B, m_C = masses of bodies A, B, C.

Note that the time derivatives indicated by the $\dot{\boldsymbol{r}}$ expressions in Eq. (1) are with respect to the inertial frame. Also, Eq. (1) assumes that the linear momentum of the system is identically zero. Using kinematic and dynamic relationships obtained from the vector diagrams and the simple rotations obtained from motions of the three gimbals, as well as the definition of the c.m., Eq. (1) is rewritten in a matrix form as

$$H_T = (I_A + I'_B + I'_C + m_B F_B + m_C F_C)\omega_A + (I'_B C_B + m_B E_B)\Omega_B + (I'_C C_C + m_C E_C)\Omega_C \tag{2a}$$

where

$$C_B = \begin{bmatrix} 0 & -\sin\alpha \\ 0 & \cos \\ 1 & 0 \end{bmatrix}, \qquad \Omega_B = \begin{bmatrix} \dot{\alpha} \\ \dot{\beta} \end{bmatrix} \tag{2b}$$

$$C_C = \begin{bmatrix} 0 & 0 \\ 1 & 0 \\ 0 & 0 \end{bmatrix}, \qquad \Omega_C = \begin{pmatrix} \dot{\gamma} \\ \dot{\phi} \end{pmatrix} \tag{2c}$$

$$D_B = \begin{bmatrix} G_{By} & -G_{Bz}\cos\alpha \\ -G_{Bx} & -G_{Bz}\sin\alpha \\ 0 & G_{By}\sin\alpha + G_{Bx}\cos\alpha \end{bmatrix}, \qquad D_C = \begin{bmatrix} -G_{Cz} & 0 \\ 0 & 0 \\ G_{Cx} & 0 \end{bmatrix} \tag{2d}$$

Table 1 Mass and inertia properties of example system

Body	Mass, lbm	I_{xx}, lbm-ft^2	I_{yy}, lbm-ft^2	I_{zz}, lbm-ft^2
A	15,000	1,218,750.0	1,218,750.0	187,500.0
B	40,000	423,333.3	423,333.3	180,000.0
C	5,000	468,646.2	406,250.0	62,500.0

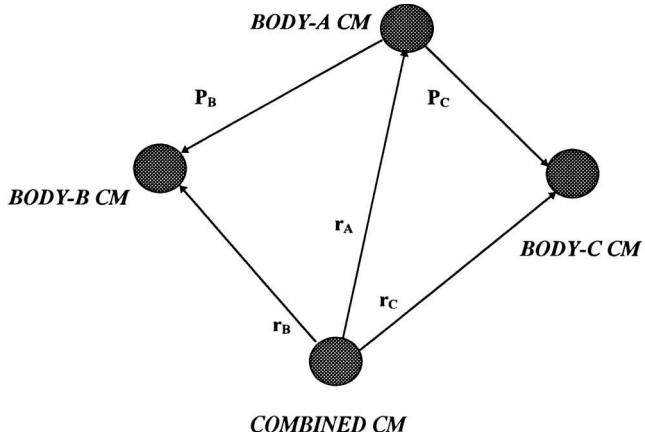

Fig. 2 Mass-center position vectors.

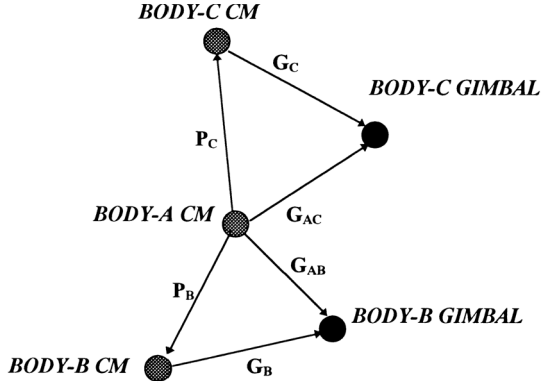

Fig. 3 Gimbal-center position vectors.

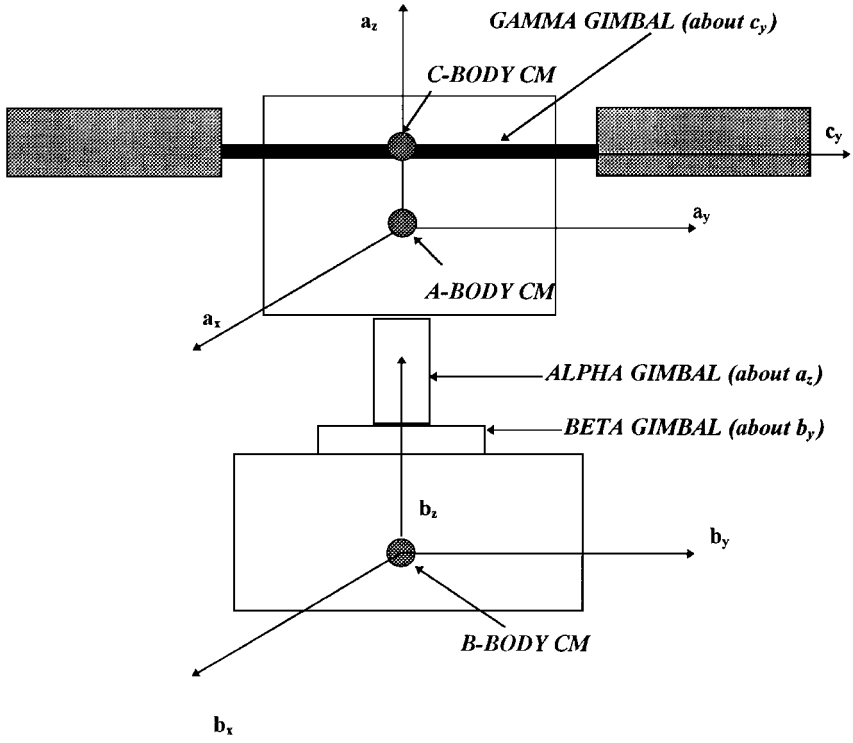

Fig. 1 Body frame and gimbal arrangements.

$$F_j = \begin{bmatrix} r_{jy}P_{jy} + r_{jz}P_{jz} & -r_{jy}P_{jx} & -r_{jz}P_{jx} \\ -r_{jx}P_{jy} & r_{jz}P_{jz} + r_{jx}P_{jx} & -r_{jz}P_{jy} \\ -r_{jx}P_{jz} & -r_{jy}P_{jz} & r_{jx}P_{jx} + r_{jy}P_{jy} \end{bmatrix} \tag{2e}$$

$$E_j = O_j D_j, \qquad O_j = \begin{bmatrix} 0 & -r_{jz} & r_{jy} \\ r_{jz} & 0 & -r_{jx} \\ -r_{jy} & r_{jx} & 0 \end{bmatrix} \tag{2f}$$

for each body j attached to body A. Referring to Fig. 3, the P and G vectors specify the locations of the body mass centers and the gimbals, respectively. Here, $j = B, C$; however, any number of additional bodies could be attached to body A via gimbals.

Note that the I'_B and I'_C matrices give the inertia properties for the bodies B and C, converted through a similarity transformation, using the appropriate direction cosine matrices, to the body A reference frame, and the F_B, F_C, C_B, C_C, E_B, and E_C matrices depend on the mass-center vectors as well as the three gimbal angles. The Ω_B and Ω_C contain the rates of the gimbals ($\dot{\phi}$ is a dummy gimbal rate). All quantities are expressed in the body A reference frame.

Equation (2) is the final form of the integral of the motion for this three-body system. It may be rewritten to solve for the angular rate $\boldsymbol{\omega}_A$ instead of the system momentum, if necessary. All of the quantities in Eq. (2) either are given in each case or are easily computed using the given information. Equation (2) is a vital component of the system simulation as well as the controller.

System Control

The main objective of this work is to develop a control scheme capable of generating a gimbal command profile to reorient the multibody system from any given initial attitude state to any desired final attitude state. The control method applied to this problem is direct collocation using nonlinear programming (DCNLP).[16] The collocation scheme requires a cost function of, among numerous other parameters, the gimbal-angle commands, which must be minimized by a numerical optimization algorithm. This minimization is accomplished by repeatedly varying the controls so that the magnitude of this function continues to decrease with each step. The resulting gimbal profile utilizes the two movable appendages to reorient the system in a specified duration.

The function to be minimized by the collocation/optimization process here is known as the total defect, represented by Δ_T. For the three-body reorientation problem studied here, the total defect is computed as a sum of the squared differences between the time derivative of the state (inertial attitude quaternion) from the differential equations of motion and a cubic estimate of the time derivative of the state, evaluated at the center of each segment. The time line is divided by N nodes into $N-1$ segments. The individual squared defects are computed for each of the segments using

$$\Delta_i = [\dot{\boldsymbol{q}}_i - \dot{\boldsymbol{q}}'_i]^2 \tag{3}$$

where $\dot{\boldsymbol{q}}_i$ is the time derivative of the attitude quaternion[19] from the differential equation of motion of a quaternion and $\dot{\boldsymbol{q}}'_i$ is the cubic estimate of the time derivative of the attitude quaternion, computed at the center of segment i. This represents a departure from the standard DCNLP method, where the defects for each segment are constrained to be zero. By removing these constraints, but minimizing the sum of the squared defects, one solves a simpler optimization problem; however, one must also then verify that the controls generated by this method produce an acceptable solution when the original equations of motion are integrated.

Note that the computation of $\dot{\boldsymbol{q}}_i$ requires knowledge of the angular rates at each segment center. These quantities are computed using Eq. (2), evaluating all parameters at the center of segment i:

$$\omega_{A,i} = (I_A + I'_B + I'_C + m_B F_B + m_C F_C)^{-1} \times [H_{T,i} - (I'_B C_B + m_B E_B)\Omega_{B,i} - (I'_C C_C + m_C E_C)\Omega_{c,i}] \tag{4}$$

Also, computation of the $\boldsymbol{q}'$ requires knowledge of the states and state rates at nodes surrounding the segment i. This is accomplished easily because the optimization routine returns the state at each node for every iteration, and the state rate can be computed using the motion equation for quaternions. The total defect then is computed as the sum of the Δ_i for all of the nodes $i = 1, N$, where N is the total number of nodes used:

$$\Delta_T = \sum_{i=1}^{N} W_i \Delta_i \tag{5}$$

where W_i is a segment-weighting term used to assign priority to the collocation conditions of a particular segment.

Equation (5) is the final form of the total defect, the function that the optimization routine must minimize by varying the control vector. The controller generates a grid of nodal information, including the controls at each node. As a check, the control was applied to Eq. (2) in a simulation code that solved for ω_A.

Results

Results have been obtained for numerous test cases involving different reorientation conditions; only a representative sample is discussed here. The quantity used predominantly to measure the extent of reorientation of a particular case is the error angle θ_E. This angle is extracted from the scalar component of the attitude quaternion and represents the total angular rotation remaining at a given time between the current actual attitude quaternion and the desired target quaternion. An alternative measure, the attitude-error difference, depicts the simple algebraic difference between the actual attitude quaternion and the target attitude quaternion, each time step. All reorientations were accomplished while constraining the gimbal positions. The gimbal rates were not constrained; however, a simple method for doing so in the zero-momentum case is depicted in a test case later. The number of nodes required to solve a reorientation problem satisfactorily depends on many different parameters particular to the conditions involved. For this work, it was most effective to use a simple process of trial and error to arrive at a number of nodes that generate a sufficient reorientation. Some experimentation with the weighting factors assigned to each segment also improved the solutions. Finally, the duration for the reorientation is a user-specified quantity. The controller will construct a reorientation sequence that is completed by any specified end time.

Figures 4 and 5 show reorientation results for a simple 20-deg yaw ($\boldsymbol{a}_z$-axis) reorientation. The initial angular rate and momentum of the system are zero. The solution was obtained using 10 nodes in the controller time line. The error angle clearly converges toward

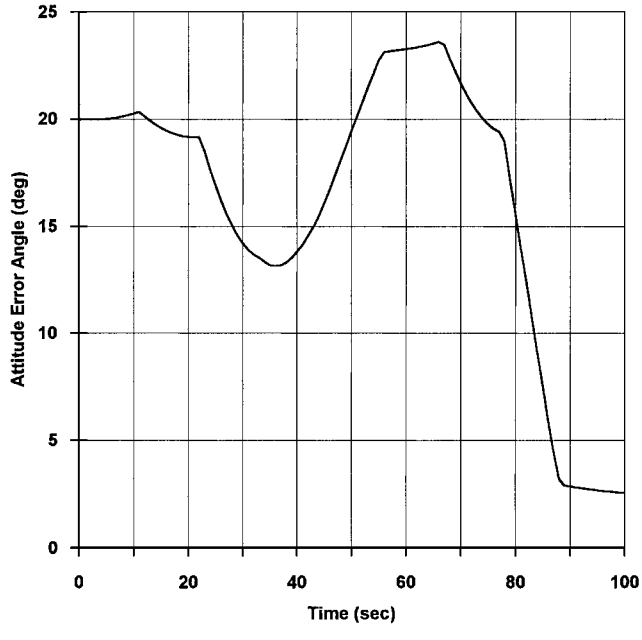

Fig. 4 Attitude-error-angle history (20-deg a_z-axis error).

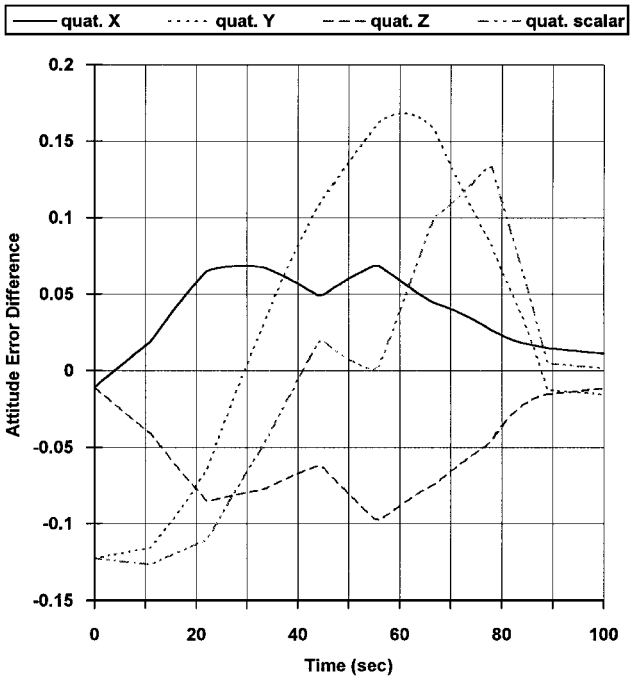

Fig. 5 Attitude-error-difference history (20-deg a_z-axis error).

0 by the end of the duration, with a residual error of approximately 2.5 deg, a reduction of nearly 90% from the initial attitude-error angle of 20 deg. The attitude-error difference plot (Fig. 5) shows all four components of the difference quaternion converging toward 0 by the end of the specified 100-s duration.

The second case involves two parts. First, we consider a reorientation of a system pitched 50 deg about the $\boldsymbol{a}_x$ axis. Again, the system's angular momentum is zero and there is no constraining of the gimbal rates. The duration for the reorientation is specified at 100 s, as before. This case required three sequential runs of the controller, each 100 s in duration and each with 12 nodes, to achieve the desired results. This was because the extent of reorientation accomplished by the first two runs was not sufficient. This was attributable to the inability of the optimization method to efficiently handle a large number of nodes because each node contributes seven parameters to the overall state vector. Each time the control algorithm was applied to the residual conditions resulting from the previous run, the final error-angle residual was reduced. This process was followed until additional runs were no longer substantially profitable. Figure 6 shows the error-angle history for this reorientation. The final residual error angle for this case was 1.1 deg, a nearly complete reorientation. In Fig. 6, error reduction resulting from each sequential maneuver is depicted, and all three maneuver sets (100 s in duration) have similar profiles. Figure 7 shows the rates at which the gimbals moved to accomplish the reorientation. From this plot, it can be seen that, at times, gimbal motion is near zero, whereas at other times the gimbal rates exceed 60 deg/s, a result of the controller design not accommodating rate constraints. This problem is remedied easily for the case of zero angular momentum by simply reconstructing the reorientation profiles such that the gimbal rates are constrained to some desired values. Given the same initial conditions as described above and the same resulting controller output, the nodal times associated with these controls were adjusted so that no gimbal rate exceeded the corresponding maximum and so that at least one gimbal rate did in fact operate at its maximum level for the duration of the segment. This is accomplished simply by dividing the required change in gimbal angle across each segment by the corresponding rate limit, for each gimbal:

$$t_\alpha = \Delta\alpha/\dot{\alpha}_{\max}, \qquad \dot{\alpha}_{\max} = 10 \text{ deg/s}$$
$$t_\beta = \Delta\beta/\dot{\beta}_{\max}, \qquad \dot{\beta}_{\max} = 10 \text{ deg/s} \tag{6}$$
$$t_\gamma = \Delta\gamma/\dot{\gamma}_{\max}, \qquad \dot{\gamma}_{\max} = 30 \text{ deg/s}$$

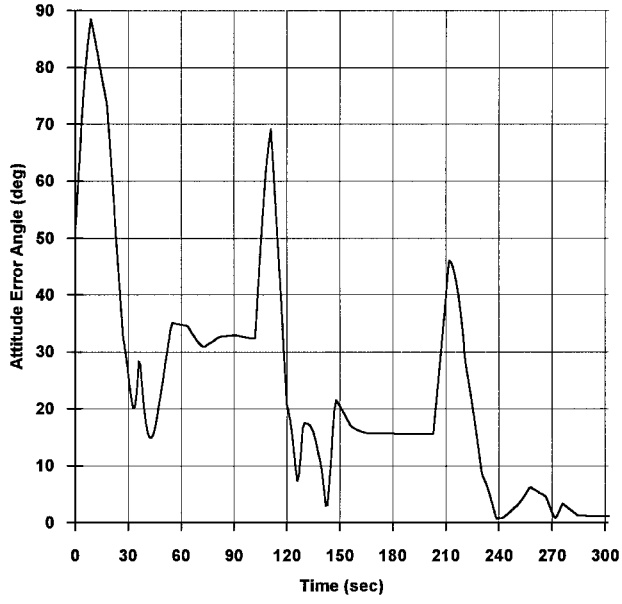

Fig. 6 Attitude-error-angle history (50-deg a_x-axis error).

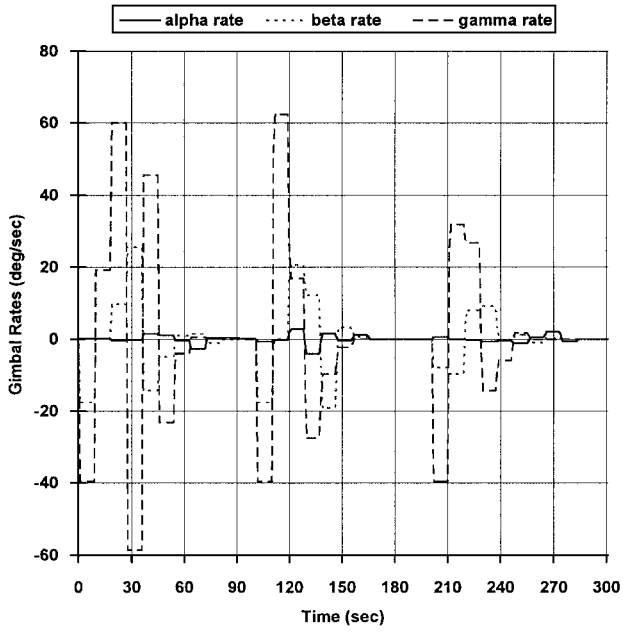

Fig. 7 Gimbal rate histories (50-deg a_x-axis error).

Then, each segment duration was taken as the maximum of the set in Eq. (6):

$$t_i = \max(t_\alpha, t_\beta, t_\gamma) \tag{7}$$

The resulting attitude-error-anglehistory is shown in Fig. 8. Notice that the profiles depicted in Figs. 6 and 8 are somewhat similar (but not identical) and the resulting error-angle residual at the conclusion of the reorientation is the same. The total duration required to achieve the 1.1-deg residual, however, is significantly different. The reduced-time reorientation required only 222 s as compared to the 300 s required for the reorientation of the unconstrained case. In addition, the gimbal rate profile now is bounded by the limits specified above. Figure 9 shows the gimbal rates for this reduced-time, constrained-rate version of the 50-deg tilt reorientation. From this figure, it can be seen that the three gimbals clearly abide by their corresponding limits. Also, note that the beta and gamma gimbals are operating at the maximum rate much of the time, resulting in a reorientation of significantly less time; however, because the objective is not a minimum-time solution, this result is merely fortuitous.

The final reorientation case to be discussed was designed to task the control method employed to its fullest extent by imposing three axes of initial attitude errors as well as three axes of initial system

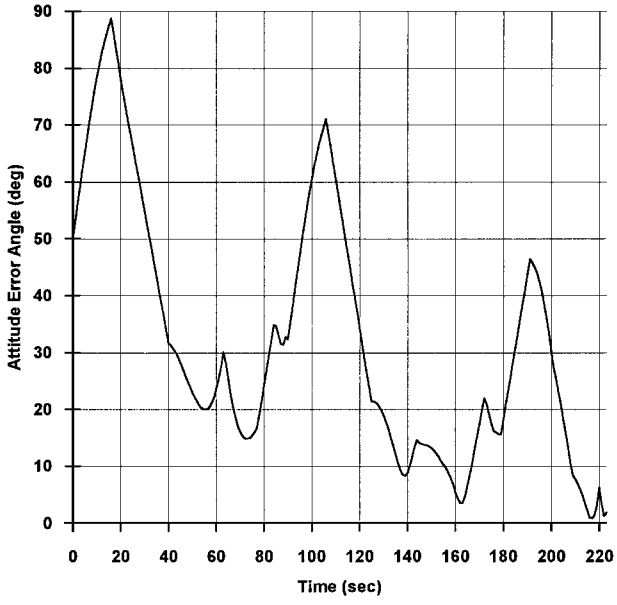

Fig. 8 Attitude-error-angle history (50-deg a_x-axis error, reduced time).

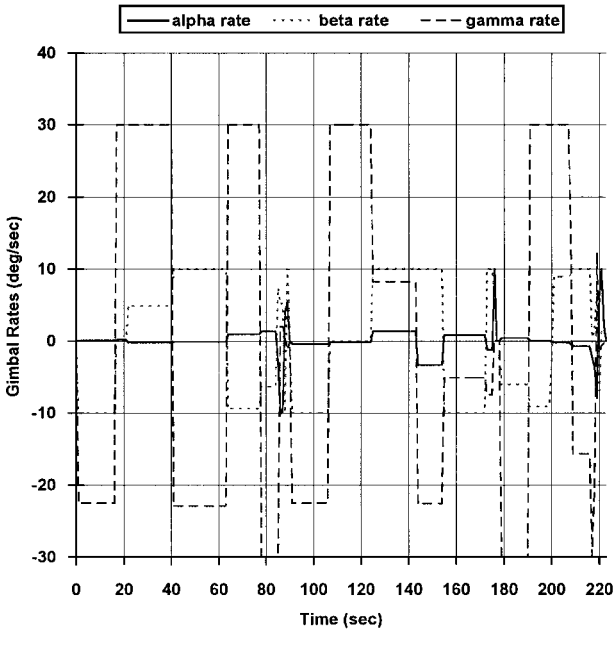

Fig. 9 Gimbal rate histories (50-deg a_x-axis error, reduced time).

rate and momentum. The system was initialized in attitude by three consecutive rotations, the first with 30 deg about the $\boldsymbol{a}_z$ axis, followed by 15 deg about the $\boldsymbol{a}_y$ axis, and, finally, 15 deg about the $\boldsymbol{a}_x$ axis. A rate of 0.01 deg/s was assigned to the $\boldsymbol{a}_x$ and $\boldsymbol{a}_y$ axes and a rate of 0.03 deg/s to the $\boldsymbol{a}_z$ axis. The attitude-error-angle history for this case is shown in Fig. 10. The reorientation required four controller runs, with nodes of 11, 12, 12, and 12, respectively, to reduce the attitude error from the initial 35-deg resultant error to 4.19 deg at the end of the 400 s. However, as Fig. 10 suggests, the first of these four sets was responsible for a very large majority of the reorientation. In the figure, the first iteration begins with a 35-deg attitude error and ends at 100 s, with a final error of about 7.5 deg. The next iteration then finishes at 200 s with 6 deg of attitude error remaining, an additional reduction of only 1 deg. The final error is 4.19 deg. Nearly 80% of the attitude maneuver was accomplished during the first iteration. Hence, the optimization routine was not capable of significant additional minimization of the cost function for the duration of the last three control sets. The rate of error reduction decreased with each maneuver set. However, the reduction of at least the first set and perhaps the second as well was quite significant, especially in light of the complex nature of the dynamics of the problem.

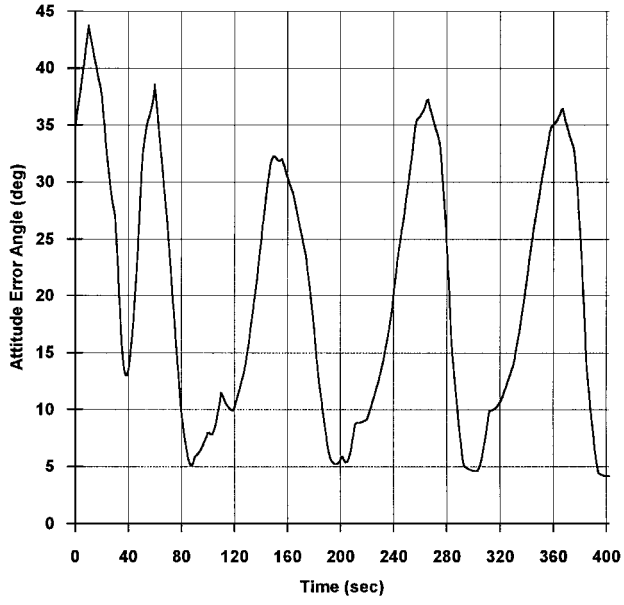

Fig. 10 Attitude-error-angle history (35-deg multiaxis error, with rate error).

Conclusions

This work has shown a feasible method for reorienting multibody spacecraft by strategically maneuvering the vehicle's appendages. A constraint can be imposed on the controller requiring that the geometric configuration of the system return to its original state before completion of the reorientation. A control algorithm was developed that was capable of commanding the movable bodies to achieve the desired reorientation. The objective was to develop an algorithm that was capable of, at a minimum, tending the system attitude in the direction of the target attitude. The results show that, for most cases, nearly complete reorientations were accomplished. A range of test cases was analyzed, covering different initial dynamic conditions. For all of the cases, the controller accomplished reorientation to within approximately 5 deg of the desired attitude. The average extent to which reorientation was accomplished was nearly 90%. That is, on average, the controller was capable of adjusting the system attitude to within 10% of the target attitude, as measured by the attitude error angle. Also, for most of the cases, the method was not sensitive to the initial guess of the states and controls, which is an additional benefit of the collocation approach. The controller showed nearly equivalent capability in reorienting systems that possessed zero or nonzero angular momentum. This is a significant component of this work because most of the previous work in this area has failed to accommodate a general state of system angular momentum. Because many spacecraft systems of this type do have nonzero inertial momentum, the generality of this solution is useful. Additionally, the algorithm developed here permits simple constraining of the gimbal-angle excursions. This results in realistic solutions to the various reorientation problems, ensuring that the commands to effect the reorientations abide by the physical limitations of the hardware involved.

References

[1] Keat, J. E., "Multibody System Order *n* Dynamics Formulation Based on Velocity Transform Method," *Journal of Guidance, Control, and Dynamics*, Vol. 13, No. 2, 1990, pp. 207–212.

[2] Grossman, R., Krishnaprasad, P. S., and Marsden, J. E., "The Dynamics of Two Coupled Rigid Bodies," *Dynamical Systems Approaches to Nonlinear Problems in Systems and Circuits*, Society for Industrial and Applied Mathematics, Philadelphia, 1988, pp. 373–378.

[3] Quartararo, R., "Two-Body Control for Rapid Attitude Maneuvers," *Advances in the Astronautical Sciences*, Vol. 42, Univelt, San Diego, CA, 1980, pp. 397–422.

[4] Sreenath, N., "Nonlinear Control of Planar Multibody Systems in Shape

Space," *Mathematics of Control, Signals, and Systems*, Vol. 5, No. 4, 1992, pp. 343–363.

[5]Enos, M. J., "On an Optimal Control Problem on $SO(3)^2$ and the Falling Cat," *Dynamics and Control of Mechanical Systems: The Falling Cat and Related Problems*, edited by M. J. Enos, American Mathematical Society, Providence, RI, 1993.

[6]Kane, T. R., and Scher, M. P., "A Dynamical Explanation of the Falling Cat Phenomenon," *International Journal of Solids and Structures*, Vol. 5, 1969, pp. 663–670.

[7]Enos, M. J., "On the Dynamics and Control of Cats, Satellites, and Gymnasts, Part II," *SIAM News*, Nov./Dec. 1992, p. 12.

[8]Alexander, S., and Park, K. C., "Minimum Torque Path Determination for Simultaneous Appendage Deployment and Satellite Attitude Reorientation," *Proceedings of the 36th AIAA/ASME/ASCE/AHS/ASC Structures, Structural Dynamics, and Materials Conference*, AIAA, Washington, DC, 1995, pp. 2474–2480 (AIAA Paper 95-1441).

[9]Patrick, G. W., "The Dynamics of Two Coupled Rigid Bodies in Three Space," *Contemporary Mathematics*, edited by J. E. Marsden, P. S. Krishnaprasad, and J. C. Simo, American Mathematical Society, Providence, RI, Vol. 97, 1989, pp. 315–335.

[10]Reyhanoglu, M., and McClamroch, N. H., "Planar Reorientation Maneuvers of Space Multibody Systems Using Internal Controls," *Journal of Guidance, Control, and Dynamics*, Vol. 15, No. 6, 1992, pp. 1475–1480.

[11]Kane, T. R., and Scher, M. P., "Human Self-Rotation by Means of Limb Movements," *Journal of Biomechanics*, Vol. 3, No. 1, 1970, pp. 39–49.

[12]Smith, P. G., and Kane, T. R., "On the Dynamics of the Human Body in Free Fall," *Journal of Applied Mechanics*, Vol. 35, No. 1, 1968, pp. 167, 168.

[13]Hussain, N. M., and Kane, T. R., "Three-Dimensional Reorientation of a System of Interconnected Rigid Bodies," *Journal of the Astronautical Sciences*, Vol. 42, No. 1, 1994, pp. 1–25.

[14]Schultz, V. H., Bock, H. G., and Longman, R. W., "Optimal Path Planning for Satellite Mounted Robot Manipulators," *Advances in the Astronautical Sciences*, Vol. 82, Univelt, San Diego, CA, 1993, pp. 311–329.

[15]Amirouche, F. M. L., *Computational Methods in Multibody Dynamics*, Prentice–Hall, Englewood Cliffs, NJ, 1992.

[16]Hargraves, C. R., and Paris, S. W., "Direct Trajectory Optimization Using Nonlinear Programming and Collocation," *Journal of Guidance, Control, and Dynamics*, Vol. 10, No. 4, 1987, pp. 338–342.

[17]Herman, A. L., and Conway, B. A., "Optimal Spacecraft Attitude Control Using Collocation and Nonlinear Programming," *Journal of Guidance, Control, and Dynamics*, Vol. 15, No. 5, 1992, pp. 1287–1289.

[18]Scrivener, S. L., "Time-Optimal Multi-Axis Attitude Maneuvers of Rigid Spacecraft Using Collocation and Nonlinear Programming," Ph.D. Thesis, Dept. of Aerospace Engineering, Pennsylvania State Univ., Dec. 1993.

[19]Wertz, J. R., *Spacecraft Attitude Determination and Control*, Reidel, Dordrecht, The Netherlands, 1978, pp. 511, 512, 758, 759.